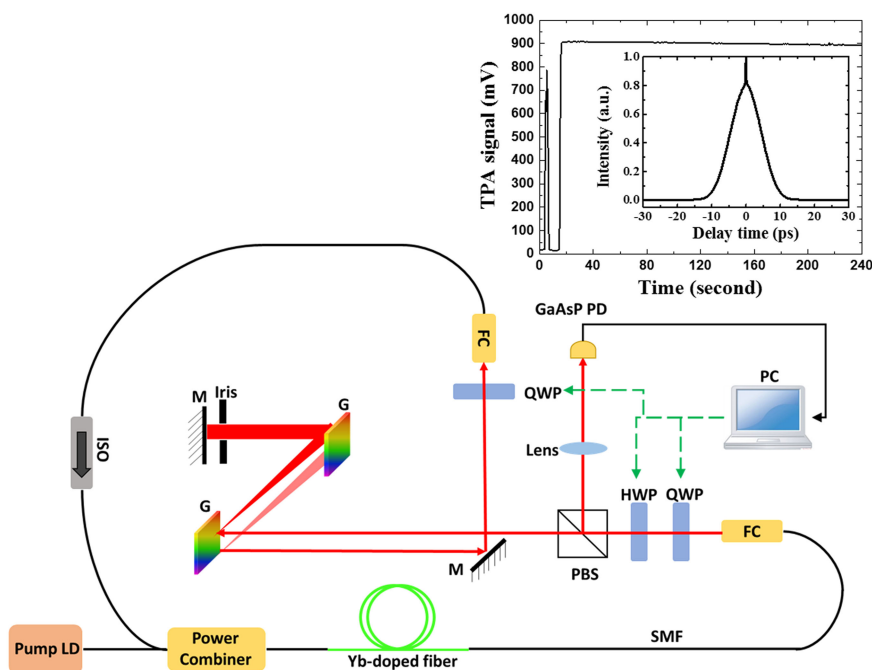# Automatic Generation of Noise-Like or Mode-Locked Pulses in an Ytterbium-Doped Fiber Laser by Using Two-Photon-Induced Current for Feedback

Hsiao-Hua Wu
Pin-Han Huang
Yuan-He Teng
Alexey Zaytsev
Osamu Wada
Ci-Ling Pan

Automatic Generation of Noise-Like or Mode-Locked Pulses in an Ytterbium-Doped Fiber Laser by Using Two-Photon-Induced Current for Feedback

Hsiao-Hua Wu [ORCID],[1] Pin-Han Huang,[2] Yuan-He Teng [ORCID],[3]
Alexey Zaytsev [ORCID],[2] Osamu Wada,[2,4] and Ci-Ling Pan [ORCID] [2,3]

[1]Department of Applied Physics, Tunghai University, Taichung 40704, Taiwan
[2]Department of Physics, National Tsing Hua University, Hsinchu 30013, Taiwan
[3]Institute of Photonics Technologies, National Tsing Hua University, Hsinchu 30013, Taiwan
[4]Center for Collaborative Research and Technology Development, Kobe University, Kobe
657-0013, Japan

Abstract: We present a simple, reliable, and fast method to automatically generate noise-like or mode-locked pulses in a fiber laser. To generate the targeted pulses, we employed two-photon-induced current from a photocell as the feedback signal to control a set of rotatable wave plates in the laser. The effectiveness of using the two-photon absorption signal to discriminate noise-like pulses from mode-locked pulses is theoretically analyzed and experimentally confirmed. We demonstrate our method by using a dispersion-mapped ytterbium-doped fiber ring laser with nonlinear polarization evolution that can generate either noise-like or mode-locked pulses. The average time to attain the prescribed pulses is within a few minutes.

Index Terms: Yb-doped fiber, mode-locked pulses, noise-like pulses, two photon absorption, automatic control.

1. Introduction

In recent years, the field of ultrafast fiber lasers [1] has experienced tremendous growth, both in terms of the science and technology as well as emergent applications. Ultrafast pulses at high average power are useful in the manufacturing industry, biomedical sensing and imaging, and as tools for studies in the fundamental science. It is generally recognized that fiber lasers will be the next wave for compact, robust, low cost, and reliable ultrafast pulse sources. Compared with state-of-art Ti: sapphire lasers, potential advantages of fiber-based laser systems include efficiency, power scaling, beam quality, ease of delivery, and low thermal budget.

Ultrafast pulsed fiber lasers can be mode-locked by using a variety of schemes, such as solitons, similaritons, and dissipative solitons [1]. A special regime of repetitively pulsed fiber laser, i.e., lasers generating the so-called noise-like pulses or NLPs [2]–[6], was also reported. The first demonstration of fiber lasers generating NLPs was that of a ring-cavity Er: doped fiber oscillator [7]. Later on, different cavity configurations and active media were employed to achieve NLPs with controllable characteristics.

A NLP is defined as some kind of complicated waveform of relatively long (sub-nanosecond) duration, within which a fine inner structure of random, much narrower sub-pulses (a few hundred femtoseconds in widths) are present. This inner structure varies from one waveform to another in the pulse train. In contrast, the mode-locked pulses (MLPs) exhibit a smooth pule profile with all the modes phase locked. The repetition rate and average duration of the aforementioned waveforms forming a train of pulses are relatively stable. Previous studies showed that NLPs have some interesting common features: (1) a very large optical bandwidth ($\sim$several tens of nanometers); (2) specific waveforms that exhibit a double-scaled average autocorrelation trace with a narrow peak riding on a wide pedestal; and (3) low temporal coherence. Moreover, it was found that NLPs are essentially undistorted even after the pulses have propagated through a lengthy dispersive medium, e.g., an optical fiber over a long distance.

Our group has successfully generated NLPs from dispersion-mapped and all-normal-dispersion or ANDi types of Yb-doped fiber lasers [8], [9]. We also demonstrated that amplified noise-like pulses could be successfully used for supercontinuum (SC) generation through standard single mode fibers (SMF) [10]. The SC spectrum is centered near 1.3 μm with a bandwidth of 420 nm. This SC source is successfully employed in a time-domain optical coherence tomography (TD-OCT) system, achieving an axial resolution of 2.3 μm. High resolution fiber-based spectral-domain OCT (SD-OCT) imaging of bio-tissue was also demonstrated [9].

In our dispersion-mapped and ANDi types of Yb-doped fiber lasers, pulses are formed using nonlinear polarization evolution (NPE) effect. These lasers are capable of operating in conventional mode-locked pulse (MLP) or NLP regime. However, the generation of the NLP or the MLP from such lasers require adjusting wave-plates to different settings and optimization. Therefore, there is a demand for a turn-key fiber laser system to automatically generate either NLPs or MLPs.

Several groups have reported automatic control of an erbium-doped fiber laser to generate MLPs. The feedback signal employed includes radio-frequency inter-mode beat spectrum [10] as well as polarization state [11]. The laser was then auto-set by tuning a liquid crystal variable retarder [10] or motorized polarization controller [11] to reach the required mode-locked regime. A more sophisticated system [12] utilized a genetic algorithm and defined a fitness function that derived from temporal and spectral output properties of the laser and attaining the target mode-locking states by means of an electronic polarization controller. Similar approaches were also employed to generate NLPs from an erbium-doped fiber laser [13], [14]. These systems usually rely on one or more expensive instruments. Attaining the required pulse output is also time-consuming. In this paper, we show that two-photon-induced current from a photodiode can effectively distinguish the NLPs from the MLPs. We construct an automatic control system by using the two-photon-induced current of a GaAsP photodiode as feedback signal to generate either NLP or MLPs from a NPE-based dispersion-mapped mode-locked ytterbium-doped fiber laser. Our system is simple, reliable, and fast.

2. Experimental Methods

A schematic of the experimental setup is shown in Fig. 1. The laser employs a 7-meter ytterbium-doped fiber (Nufern, LMA-YDF-10/125-9M) as the gain medium. The NPE port consists of free space polarization controllers (two quarter-wave plates and a half-wave plate) mounted on electrically-driven rotating stages (Thorlabs, KPRM1E) as well as a polarization beam splitter (Newport, 05FC16PB.7). A 915 nm laser diode (SkyEra, TY91510W01) is used for pumping. The dispersion map scheme consists of a pair of diffraction gratings (Thorlabs, GR65-0610) in a near Littrow configuration which introduces the negative group delay dispersion (GDD) to the laser cavity
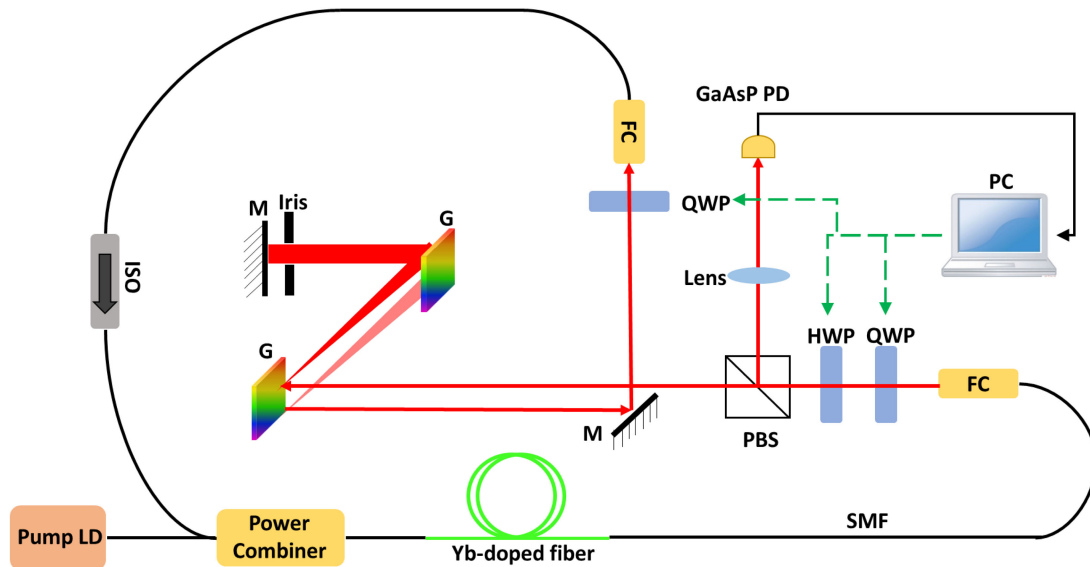
Fig. 1. Schematic setup of the fiber laser system. FC, fiber coupler; G, grating; HWP, half-wave plate; QWP, quarter-wave plate; PBS, polarization beam splitter; M, mirror; LD, laser diode; PC, personal computer.

and an iris which is used as a tunable filter to select the central wavelength and optical bandwidth of the optical pulses. Two fiber couplers are employed for coupling the laser beam from one end of the fiber cavity to free space and return to the other end of the fiber cavity, respectively. An optical isolator is placed right after the fiber coupler to ensure unidirectional operation of the laser. Such an arrangement facilitates self-starting of the mode-locking process. The laser is out-coupled from the reflection port of the polarization beam splitter.

Our laser can operate in various regimes, i.e., continuous wave, the NLP mode locking, single-pulse mode locking, multi-pulse mode locking, harmonic mode-locking, etc., at different pump powers and NPE settings.

In this work, we focus on studies of the generation of the NLPs and the single-pulse MLPs. At a particular pump power, by adjusting three wave plates to certain combinations of orientations, we can observe either NLPs or MLPs. Usually, single-pulse mode locking can only be observed at low pump power (below 1.3 W in this laser). Higher pump power will result in pulse splitting or even harmonic mode locking. The NLP mode-locking regime also occurs at higher pump powers. Fig. 2(a) illustrates the various operating regime of our laser. For NLP operation, the spectra are similar, with bandwidth vary from 54 to 61 nm as the pump power was increased from ∼1.7 W to 2.6 W (see Fig. 2(b)).

Typical pulse trains, autocorrelation traces, and optical spectra for NLPs and MLPs are shown in Fig. 3. We can see that the NLPs exhibit irregular pulse amplitude, femtosecond/picosecond double-scaled intensity autocorrelation (IAC) traces and broader spectrum than that of the MLP. For the data shown in Fig. 3, the NLP exhibits a spike width of 350 fs and pedestal width of 10 ps (Gaussian fitting). The ratio between the peak intensity and that of the shoulder in Fig. 3(b) is ∼1.32. The optical bandwidth of the NLP is 50 nm. In contrast, the duration of the MLPs is 6 ps (Gaussian fitting) and the optical bandwidth is 14 nm. So, the corresponded "single-pulse" durations can be estimated as ∼7ps for NLP and ∼4ps for MLP, respectively.

The wave-plates are first set to random orientations prior to the automatic control experiment. We then rotate the first quarter-wave plate, the half-wave plate and the second quarter-wave plate in sequence to generate the NLP or the MLP by means of the NPE effect. For feedback and auto-setting, we used a GaAsP photodiode (Hamamatsu G1117) whose bandgap energy is larger than the photon energy of the laser at wavelength around 1070 nm, with a spectral response range
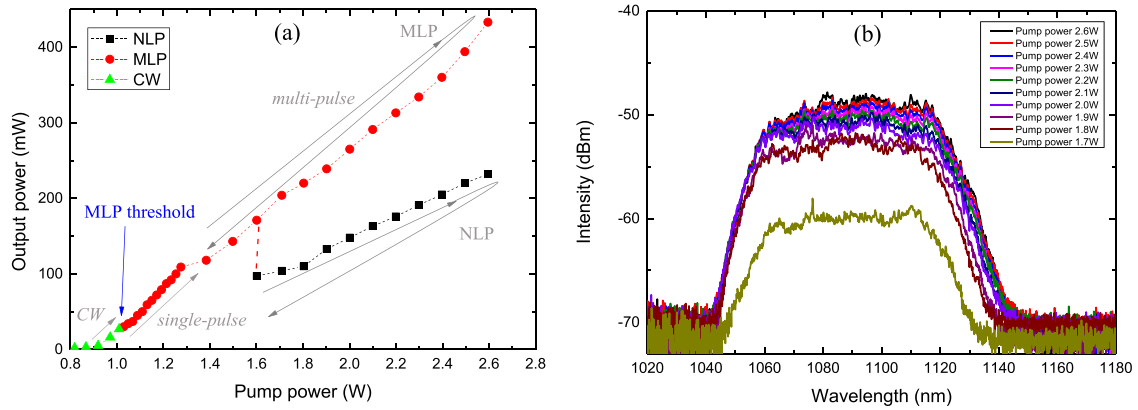
Fig. 2. (a) Operating regime of the laser as a function of pump power. CW, continuous wave; (b) Output spectra of the Laser operating in NLP mode. Traces of different color correspond to different pump power.
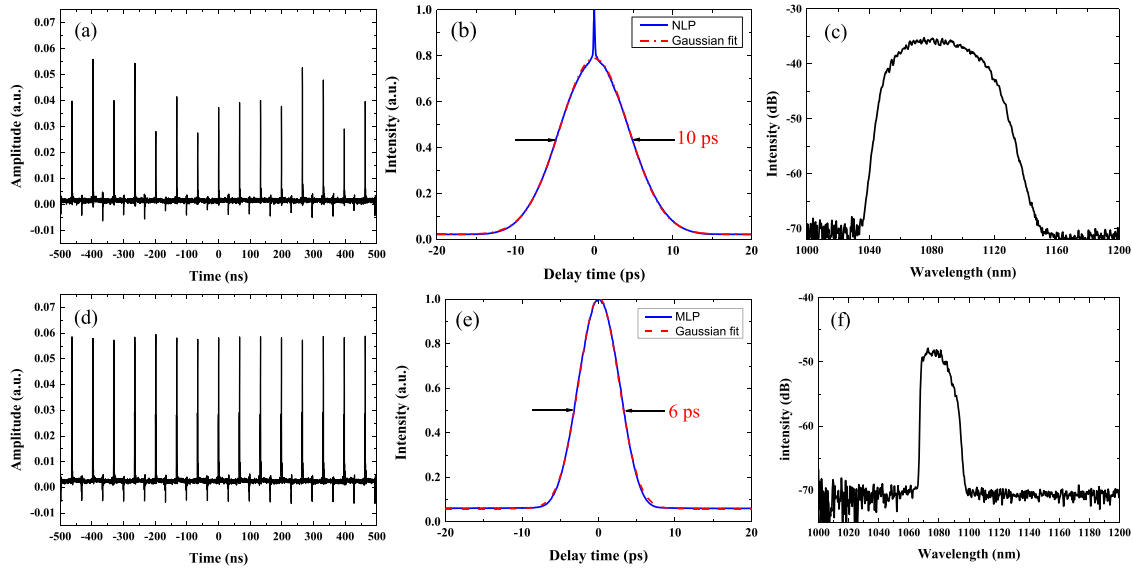

Fig. 3. Oscilloscope traces of the pulse trains, autocorrelation traces, and optical spectra of the laser operating in NLP (a, b, c) and (single-pulse) MLP (d, e, f) modes.

of ~300 – 680 nm. The photodiode, therefore, detects laser pulses and generates corresponding photocurrent mainly by means of the two-photon absorption (TPA) effect. As shown in the next section, Magnitudes of the TPA signal due to the laser generating NLPs or MLPs are significantly different. Thus, one can set the appropriate TPA signal and adjust orientations of three wave plates which were mounted on motorized rotation stages accordingly. The laser can then generate either MLPs or NLPs automatically.

3. Theoretical Analysis

The carrier generation rate due to TPA in a photodiode illuminated by laser pulses can be written as [15]

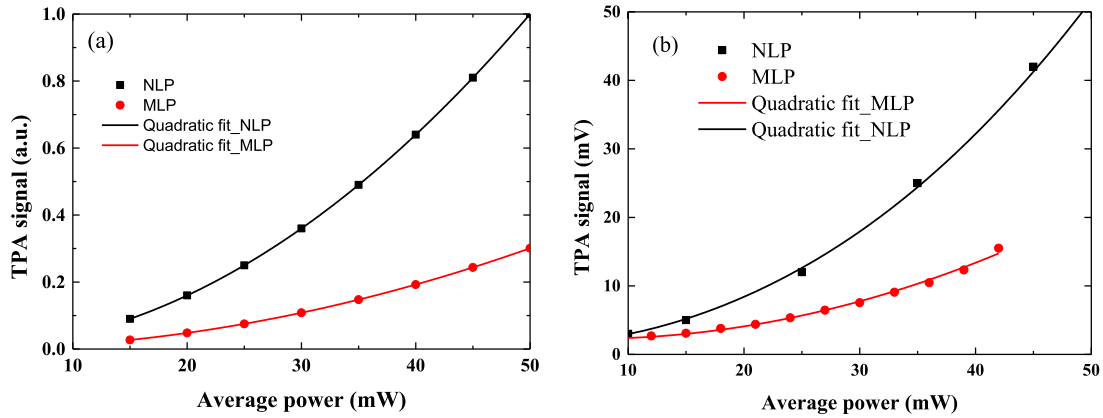$$\frac{dN_{2p}}{dt} = \frac{\beta_2}{2E_P}I^2(t), \tag{1}$$

Fig. 4. The quadratic dependence of TPA signal as a function of the average power for the NLP and the MLP by (a) theoretical simulation and (b) experiment.
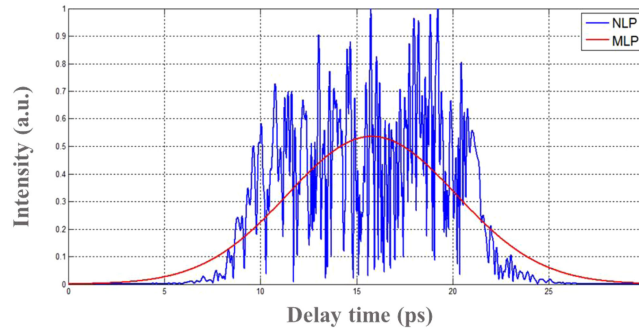

Fig. 5. Examples of simulated NLP and MLP waveforms of equal pulse energies and similar durations. NLP: noise-like pulses, MLP: mode-locked pulse.

where N_{2p} is the photogenerated carrier density induced by TPA, β_2 is the TPA coefficient, E_p is the photon energy and I(t) is the time-dependent irradiance of laser pulses. The TPA-induced photocurrent of a photodiode is proportional to the N_{2p} and the photocurrent can be calculated as

$$J = \frac{1}{T} \int_{-T/2}^{T/2} \frac{\beta_2}{2E_P} I^2(t)dt, \tag{2}$$

where T is the integration time of the detection system.

To calculate the TPA-induced photocurrent, we assume a Gaussian pulse waveform $I(t) = \exp(-(t/\tau)^2 \, 4 \ln 2)$ with duration $\tau = 4$ ps for MLPs. The NLPs are constructed by assuming that each NLP bunch consisting of stochastic delta-function-like spikes with random time delay between them and random relative phases with a Gaussian envelope consistent with experimentally observed IAC traces [16]. The durations for spikes and the envelope used in the simulation after autocorrelation are 350 femtoseconds and 10 picoseconds, respectively. For the purpose of comparison, we set the pulse energies of MLPs and the NLPs to be the average of 50 pulses.

The theoretically calculated TPA signals as a function of the average power of our laser generating NLPs and MLPs are shown in Fig. 4 (a).

Somewhat surprisingly, we find that the NLPs generate higher TPA signals than the MLPs with pulse width similar to the waveform duration of the single NLP at the same average power. This is confirmed by experimental measurement as shown in Fig. 4 (b). To explain, we plot examples of simulated NLP and MLP waveforms of equal pulse energies and similar durations in Fig. 5. It is
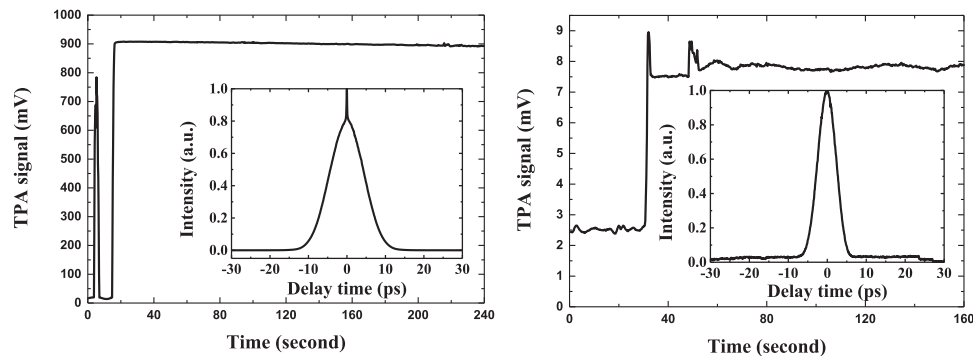
Fig. 6. TPA signals versus time for (a) the NLP and (b) the MLP. The insets are respectively their autocorrelation traces.

very clear that the peak intensities attributed to the stochastic spikes of the NLP reach much larger values than that of the MLP. Conceivably, the collection of random femtosecond spikes within each NLP bunch contribute to the observed effect. The TPA signal is therefore an effective parameter to discriminate the NLP from the MLP. In the experiment, the regime of single-pulse mode-locking is represented by the case in which the pump power of 1.1 W (See Fig. 2(a)). The average output power of the laser was 42 mW while the corresponding TPA signal was 15 mV. For the NLP case, we operated the laser at a pump power of 2 W. The average output power of the laser was 198 mW and the corresponding TPA signal was 928 mV. A variable attenuator was employed to ensure that the average power of the laser operating in the two regimes reaching the detector are the same for the data shown in Fig. 4.

It could be argued that experimentally observed difference in TPA signal could be caused by the spectrum difference of NLP and MLP. The TPA coefficient, β_2 in Eqs. 1 and 2, is wavelength dependent. Typically it reaches the maximum at a wavelength corresponds to $0.7E_g$, where E_g is the bandgap energy of the semiconductor. The GaAsP photodiode we employed has a cut-off of $\sim$680 nm, suggesting that its photosensitive layer is probably $GaAs_{0.55}P_{0.45}$, with a band gap energy of $E_g = 1.98$ eV. The wavelength corresponds to $0.7E_g$ is $\sim$0.89 μm. This is out of the emission wavelength range of our laser either in either the NLP or MLP mode. Moreover, we have generated NLPs with narrower spectral bandwidth ($\sim$18 nm) as opposed to 50 - 60 nm of the regime reported Fig. 2. The TPA signal for NLPs in this case is still greater than that for MLP. Therefore, the mentioned resonant TPA effect probably played a minor role in the observed phenomena.

4. Results and Discussion

As discussed in Sec. 3, the TPA signal is related to states (the MLP or the NLP) of the laser at a given pump power as shown in Fig. 4 (b). In this work, we let the wave-plates rotating to different settings until the TPA signal reaches the target value. In this fashion, we can control the laser to generate either the NLP or the MLP.

As one might expect, the final TPA signal is related to the laser output power. For example, when the final TPA signal was increased from 865 mV to 1500 mV, the average laser power increased from 178 mW to 235 mW at a pump power of 2 W. In addition, the spike to shoulder ratio changed from 1.74 to 1.19. By setting the magnitude and the permitted range of variation for TPA signal to required values, the system can self-search and generate the prescribed laser pulses. After the prescribed pulse is attained, the TPA signal from the photodiode is still monitored. If it is out of the preset range, the wave-plates will restart to rotate until the prescribed TPA signal is reached again. Typical time evolution of TPA signals and the autocorrelation traces of the generated NLP and MLP are shown in Fig. 6 (a) and (b) and insets, respectively. The time to search and acquire the NLP or MLP is usually around a few minutes. The time to search and acquire the NLP or MLP is mainly
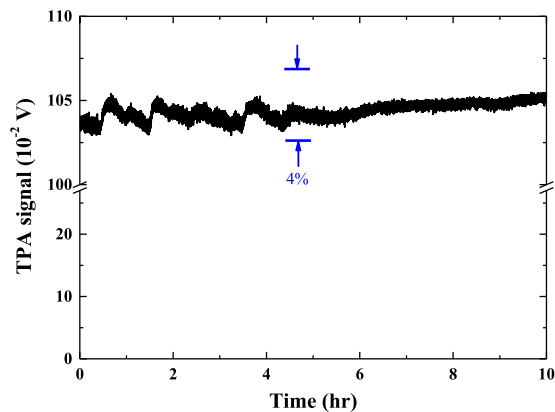
Fig. 7. TPA signals versus time for NLPs.

limited by the mechanical movement of the stages used for rotating the waveplates. It could be improved when the motor-driven stages are replaced by faster devices such as the liquid crystal phase retarders or the electronic polarization controllers. Machine-learning-based algorithm could speed up the process.

Our laser system can be set to generate stable NLPs over an extended period of time. The servo loop usually does not need to be reset for a few day unless mode locking is forced to break by blocking the light path in the cavity. This is also the method we used to demonstrate the reset function of the automatically controlled laser system. This is illustrated in Fig. 7, in which the variation of TPA signal is shown to be less than 4% peak-to-peak over a period of 10 hours. The NLPs exhibit irregular pulse amplitude and multiple random spikes which are distributed within a time interval approximately corresponding to the pedestal width of the autocorrelation trace (See Fig. 5). The phase noise, amplitude jitter, and timing jitter of the NLPs are therefore expected to be worse than that of the MLPs.

5. Conclusion

We present a simple, reliable and fast method to automatically generate noise-like or mode-locked pulses in a fiber laser. To generate the targeted pulses, we employed two-photon-induced current from a photocell as the feedback signal to control a set of rotatable wave-plates. The effectiveness of using the two-photon absorption signal to discriminate noise-like pulses from mode-locked pulses is theoretically analyzed and experimentally confirmed. We demonstrate our method by using a dispersion-mapped ytterbium-doped fiber ring laser with nonlinear polarization evolution port that can generate either noise-like or mode-locked pulses Average time to attain the prescribed pulses is typically a few minutes. Once the NLP is generated, it can persist over a few days exhibiting very good long term stability. We also find that higher target TPA signal will result in higher average power in the laser output. The time for tracking and forming the target pulses can be further shortened when the liquid crystal phase retarder or the electronic polarization controller is employed in place of the motor-driven mechanically rotating wave-plates employed in this work. The TPA signal is proportional to peak irradiance of optical pulses regardless of the underlying mechanisms for pulse formation. The present approach is thus potentially applicable for autosetting of other mode-locked laser systems.

Acknowledgment

References

[1] M. E. Fermann and I. Hart, "Ultrafast fibre lasers," *Nature Photon.*, vol. 7, pp. 868–874, 2013.

[2] O. Pottiez, R. Grajales-Coutino, B. Ibarra-Escamilla, E. A. Kuzin, and J. C. Hernandez-Garcia, "Adjustable noiselike pulses from a figure-eight fiber laser," *Appl. Opt.*, vol. 50, no. 25, pp. E24–E31, 2011.

[3] S. Kobtsev, S. Kukarin, S. Smirnov, S. Turitsyn, and A. Latkin, "Generation of double-scale femto/pico-second optical lumps in mode-locked fiber lasers," *Opt. Exp.*, vol. 17, no. 23, pp. 20707–20713, 2009.

[4] Y. An, D. Shen, W. Zhao, and J. Long, "Characteristics of pulse evolution in mode-locked thulium-doped fiber laser," *Opt. Commun.*, vol. 285, no. 7, pp. 1949–1953, 2012.

[5] S. Kobtsev and S. Smirnov, "Fiber lasers mode-locked due to nonlinear polarization evolution: Golden mean of cavity length," *Laser Phys.*, vol. 21, no. 2, pp. 272–276, 2011.

[6] L. M. Zhao, D. Y. Tang, J. Wu, X. Q. Fu, and S. C. Wen, "Noise-like pulse in a gain-guided soliton fiber laser," *Opt. Exp.*, vol. 15, no. 5, pp. 2145–2150, 2007.

[7] M. Horowitz, Y. Barad, and Y. Silberberg, "Noiselike pulses with a broadband spectrum generated from an erbium-doped fiber laser," *Opt. Lett.*, vol. 22, no. 11, pp. 799–801, 1997.

[8] A. K. Zaytsev, C. H. Lin, Y. J. You, F. H. Tsai, C. L. Wang, and C. L. Pan, "Controllable noise-like operation regime in Yb: Doped dispersion-mapped fiber ring laser," *Laser Phys. Lett.*, vol. 10, no. 4, 2013, Art. no. 045104.

[9] Y. J. You, C. M. Wang, Y. L. Lin, A. Zaytsev, P. Xue, and C. L. Pan, "Ultrahigh-resolution optical coherence tomography at 1.3 μm central wavelength by using a supercontinuum source pumped by noise-like pulses," *Laser Phys. Lett.*, vol. 13, no. 2, 2016, Art. no. 025101.

[10] A. Zaytsev, C. H. Lin, Y. J. You, C. C. Chung, C. L. Wang, and C. L. Pan, "Supercontinuum generation by noise-like pulses transmitted through normally dispersive standard single-mode fibers," *Opt. Exp.*, vol. 21, no. 13, pp. 16056–16062, 2013.

[11] M. Olivier, M.-D. Gagnon, and M. Piché, "Automated mode locking in nonlinear polarization rotation fiber lasers by detection of a discontinuous jump in the polarization state," *Opt. Exp.*, vol. 23 no. 5, pp. 6738–6746, 2015.

[12] R. I. Woodward and E. J. R. Kelleher, "Towards 'smart lasers': Self-optimisation of an ultrafast pulse source using a genetic algorithm," *Sci. Rep.*, vol. 6, 2016, Art. no. 37616.

[13] U. Andral *et al.*, "Toward an autosetting mode-locked fiber laser cavity," *J. Opt. Soc. Amer. B*, vol. 33, no. 5, pp. 825–833, 2016.

[14] U. Andral, R. Si Fodil, F. Amrani, F. Billard, E. Hertz, and P. Grelu, "Fiber laser mode-locked through an evolutionary algorithm," *Optica*, vol. 2, no. 4, pp. 275–278, 2015.

[15] F. R. Laughton, J. H. Marsh, D. A. Barrow, and E. L. Portnoi, "The two-photon absorption semiconductor waveguide autocorrelator," *IEEE J. Quantum Electron.*, vol. 30, no. 3, pp. 838–845, Mar. 1994.

[16] A. Boucon *et al.*, "Noise-like pulses generated at high harmonics in a partially-mode-locked km-long Raman fiber laser," *Appl. Phys. B*, vol. 106, no. 2, pp. 283–287, 2012.